

RETCL: A Selection-based Approach for Retrosynthesis via Contrastive Learning

Hankook Lee^{1*} Sungsoo Ahn² Seung-Woo Seo³ You Young Song⁴
Eunho Yang¹⁵ Sung-Ju Hwang¹⁵ Jinwoo Shin¹

¹Korea Advanced Institute of Science and Technology (KAIST)

²Mohamed bin Zaeyed University of Artificial Intelligence

³Standigm ⁴Samsung Electronics ⁵AITRICS

Abstract

Retrosynthesis, of which the goal is to find a set of reactants for synthesizing a target product, is an emerging research area of deep learning. While the existing approaches have shown promising results, they currently lack the ability to consider availability (e.g., stability or purchasability) of the reactants or generalize to unseen reaction templates (i.e., chemical reaction rules). In this paper, we propose a new approach that mitigates the issues by reformulating retrosynthesis into a selection problem of reactants from a candidate set of commercially available molecules. To this end, we design an efficient reactant selection framework, named RETCL (retrosynthesis via contrastive learning), for enumerating all of the candidate molecules based on selection scores computed by graph neural networks. For learning the score functions, we also propose a novel contrastive training scheme with hard negative mining. Extensive experiments demonstrate the benefits of the proposed selection-based approach. For example, when all 671k reactants in the USPTO database are given as candidates, our RETCL achieves top-1 exact match accuracy of 71.3% for the USPTO-50k benchmark, while a recent transformer-based approach achieves 59.6%. We also demonstrate that RETCL generalizes well to unseen templates in various settings in contrast to template-based approaches.

1 Introduction

Retrosynthesis (Corey, 1991), finding a synthetic route starting from commercially available reactants to synthesize a target product (see Figure 1a), is at the center of focus for discovering new materials in both academia and industry. It plays an essential role in practical applications by finding a new synthetic path, which can be more cost-effective or avoid patent infringement. However, retrosynthesis is a challenging task that requires searching over a vast number of molecules and chemical reactions, which is intractable to enumerate. Nevertheless, due to its utter importance, researchers have developed computer-aided frameworks to automate the process of retrosynthesis for more than three decades (Corey et al., 1985).

*This work was partially done while the first author visited Samsung Advanced Institute of Technology (SAIT).

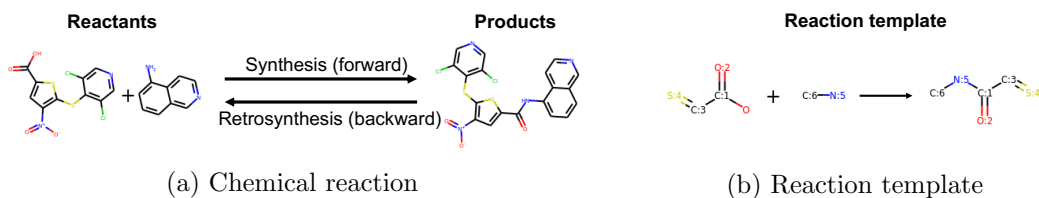


Figure 1: Examples of (a) a chemical reaction and (b) the corresponding reaction template in the USPTO-50k dataset. The objective of retrosynthesis is to find the reactants for the given product.

The computer-aided approaches for retrosynthesis mainly fall into two categories depending on their reliance on the reaction templates, i.e., sub-graph patterns describing how the chemical reaction occurs among reactants (see Figure 1b). The template-based approaches (Coley et al., 2017b; Segler & Waller, 2017; Dai et al., 2019) first enumerate known reaction templates and then apply a well-matched template into the target product to obtain reactants. Although they can provide chemically interpretable predictions, they limit the search space to known templates and cannot discover novel synthetic routes. In contrast, template-free approaches (Liu et al., 2017; Karpov et al., 2019; Zheng et al., 2019; Shi et al., 2020) generate the reactants from scratch to avoid relying on the reaction templates. However, they require to search the entire molecular space, and their predictions could be either unstable or commercially unavailable.

We emphasize that retrosynthesis methods are often required to consider the availability of reactants and generalize to unseen templates in real-world scenarios. For example, when a predicted reactant is not available (e.g., not purchasable) for a chemist or a laboratory, the synthetic path starting from the predicted reactant cannot be instantly used in practice. Moreover, chemists often require retrosynthetic analysis based on unknown reaction rules. This is especially significant due to our incomplete knowledge of chemical reactions; e.g., 29 million reactions were regularly recorded between 2009 and 2019 in Reaxys¹ (Mutton & Ridley, 2019).

Contribution. In this paper, we propose a new *selection-based* approach, which allows considering the commercial availability of reactants. To this end, we reformulate the task of retrosynthesis as a problem where reactants are selected from a candidate set of available molecules. This approach has two benefits over the existing ones: (a) it guarantees the commercial availability of the selected reactants, which allows chemists proceeding to practical procedures such as lab-scale experiments or optimization of reaction conditions; (b) it can generalize to unseen reaction templates and find novel synthetic routes.

For the selection-based retrosynthesis, we propose an efficient selection framework, named RETCL (retrosynthesis via contrastive learning). To this end, we design two effective selection scores in synthetic and retrosynthetic manners. To be specific, we use the cosine similarity between molecular embeddings of the product and the reactants computed by graph neural networks. For training the score functions, we also propose a novel contrastive learning scheme (Sohn, 2016; He et al., 2019; Chen et al., 2020b) with hard negative mining (Harwood et al., 2017) to overcome a scalability issue while handling a large-scale candidate set.

¹A chemical database, <https://www.reaxys.com>

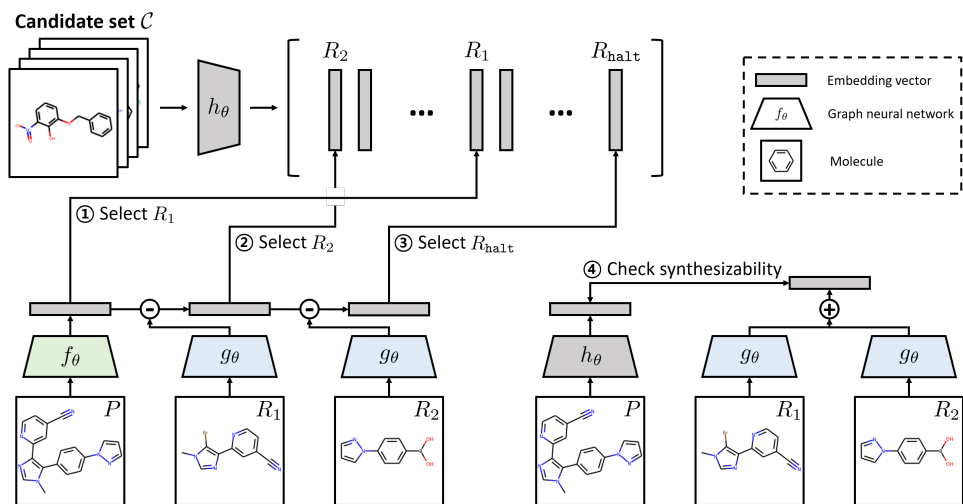


Figure 2: Illustration of the search procedure in RETCL. It first (1-3) selects reactants sequentially based on $\psi(R|P, \mathcal{R}_{\text{given}})$, and then (4) check the synthesizability of the selected reactant-set based on $\phi(P|\mathcal{R})$. The overall score is the average over all scores from (1) to (4).

To demonstrate the effectiveness of our RETCL, we conduct various experiments based on the USPTO database (Lowe, 2012) containing 1.8M chemical reactions in the US patent literature. Thanks to our prior knowledge on the candidate reactants, our method achieves 71.3% test accuracy and significantly outperforms the baselines without such prior knowledge. Furthermore, our algorithm demonstrates its superiority even when enhancing the baselines with candidate reactants, e.g., our algorithm improves upon the existing template-free approach (Chen et al., 2019) by 11.7%. We also evaluate the generalization ability of RETCL by testing USPTO-50k-trained models on the USPTO-full dataset; we obtain 39.9% test accuracy while the state-of-the-art template-based approach (Dai et al., 2019) achieves 26.7%. Finally, we demonstrate how our RETCL can improve multi-step retrosynthetic analysis where intermediate reactants are not in our candidate set.

We believe our scheme has the potential to improve further in the future, by utilizing (a) additional chemical knowledge such as atom-mapping or leaving groups (Shi et al., 2020; Somnath et al., 2020); (b) various contrastive learning techniques in other domains, e.g., computer vision (He et al., 2019; Chen et al., 2020b; Hénaff et al., 2019; Tian et al., 2019), audio processing (Oord et al., 2018), and reinforcement learning (Srinivas et al., 2020).

2 Selection-based retrosynthesis via contrastive learning

2.1 Overview of RetCL

In this section, we propose a selection framework for retrosynthesis via contrastive learning, coined RETCL. Our framework is based on solving the retrosynthesis task as a selection problem over a candidate set of *commercially available reactants* given the target product. Especially, we design a selection procedure based on molecular embeddings computed by graph neural networks and train the networks via contrastive learning.

To this end, we define a chemical reaction $\mathcal{R} \rightarrow P$ as a synthetic process of converting a

reactant-set $\mathcal{R} = \{R_1, \dots, R_n\}$, i.e., a set of *reactant* molecules, to a *product* molecule P (see Figure 1a). We aim to solve the problem of retrosynthesis by finding the reactant-set \mathcal{R} from a *candidate set* \mathcal{C} which can be synthesized to the target product P . Especially, we consider the case when the candidate set \mathcal{C} consists of *commercially available* molecules. Throughout this paper, we say that the synthetic direction (from \mathcal{R} to P) is *forward* and the retrosynthetic direction (from P to \mathcal{R}) is *backward*.

Note that our framework stands out from the existing works in terms of the candidate set \mathcal{C} . To be specific, (a) template-free approaches (Lin et al., 2019; Karpov et al., 2019; Shi et al., 2020) choose \mathcal{C} as the whole space of (possibly unavailable) molecules; and (b) template-based approaches (Coley et al., 2017b; Segler & Waller, 2017; Dai et al., 2019) choose \mathcal{C} as possible reactants extracted from the known reaction templates. In comparison, our framework neither requires (a) search over the entire space of molecules, or (b) domain knowledge to extract the reaction templates.

We now briefly outline the RETCL framework. Our framework first searches the most likely reactant-sets $\mathcal{R}_1, \dots, \mathcal{R}_T \subset \mathcal{C}$ in a sequential manner based on a backward selection score $\psi(R|P, \mathcal{R}_{\text{given}})$, and then ranks the reactant-sets using $\psi(R|P, \mathcal{R}_{\text{given}})$ and another forward score $\phi(P|\mathcal{R})$. For learning the score functions, we propose a novel contrastive learning scheme with hard negative mining for improving the selection qualities. We next provide detailed descriptions of the search procedure and the training scheme in Section 2.2 and 2.3, respectively.

2.2 Search procedure with graph neural networks

We first introduce the search procedure of RETCL in detail. To find a reactant-set $\mathcal{R} = \{R_1, \dots, R_n\}$, we select each element R_i sequentially from the candidate set \mathcal{C} based on the *backward* (retrosynthetic) selection score $\psi(R|P, \mathcal{R}_{\text{given}})$. It represents a selection score of a reactant R given a target product P and a set of previously selected reactants $\mathcal{R}_{\text{given}} \subset \mathcal{C}$. Note that the score function is also capable of selecting a special reactant R_{halt} to stop updating the reactant-set. Using beam search, we choose top T likely reactant-sets $\mathcal{R}_1, \dots, \mathcal{R}_T$.

Furthermore, we rank the chosen reactant-sets $\mathcal{R}_1, \dots, \mathcal{R}_T$ based on the backward selection score $\psi(R|P, \mathcal{R}_{\text{given}})$ and the *forward* (synthetic) score $\phi(P|\mathcal{R})$. The latter represents the synthesizability of \mathcal{R} for P . Note that $\psi(R|P, \mathcal{R}_{\text{given}})$ and $\phi(P|\mathcal{R})$ correspond to backward and forward directions of a chemical reaction $\mathcal{R} \rightarrow P$, respectively (see Section 2.1 and Figure 1a). Using both score functions, we define an overall score on a chemical reaction $\mathcal{R} \rightarrow P$ as follows:

$$\text{score}(P, \mathcal{R}) = \frac{1}{n+2} \left(\max_{\pi \in \Pi} \sum_{i=1}^{n+1} \psi(R_{\pi(i)}|P, \{R_{\pi(1)}, \dots, R_{\pi(i-1)}\}) + \phi(P|\mathcal{R}) \right), \quad (1)$$

where $R_{n+1} = R_{\text{halt}}$ and Π is the space of permutations defined on the integers $1, \dots, n+1$ satisfying $\pi(n+1) = n+1$. Based on $\text{score}(P, \mathcal{R})$, we decide the rankings of $\mathcal{R}_1, \dots, \mathcal{R}_T$ for synthesizing the target product P . We note that the $\max_{\pi \in \Pi}$ operator and the $\frac{1}{n+2}$ term make the overall score (equation 1) be independent of order and number of reactants, respectively. Figure 2 illustrates this search procedure of our framework.

Score design. We next elaborate our design choices for the score functions ψ and ϕ . We first observe that the molecular graph of the product P can be decomposed into subgraphs

from each reactant of the reactant-set \mathcal{R} , as illustrated in Figure 1a. Moreover, when selecting reactants sequentially, the structural information of the previously selected reactants $\mathcal{R}_{\text{given}}$ should be ignored to avoid duplicated selections. From these observations, we design the scores $\psi(R|P, \mathcal{R}_{\text{given}})$ and $\phi(P|\mathcal{R})$ as follows:

$$\begin{aligned}\psi(R|P, \mathcal{R}_{\text{given}}) &= \text{CosSim} \left(f_{\theta}(P) - \sum_{S \in \mathcal{R}_{\text{given}}} g_{\theta}(S), h_{\theta}(R) \right), \\ \phi(P|\mathcal{R}) &= \text{CosSim} \left(\sum_{R \in \mathcal{R}} g_{\theta}(R), h_{\theta}(P) \right),\end{aligned}$$

where CosSim is the cosine similarity and f_{θ} , g_{θ} , h_{θ} are embedding functions from a molecule to a fixed-sized vector with parameters θ . Note that one could think that f_{θ} and g_{θ} are query functions for a product and a reactant, respectively, while h_{θ} is a key function for a molecule. Such a query-key separation allows the search procedure to be processed as an efficient matrix-vector multiplication. This computational efficiency is important in our selection-based setting because the number of candidates is often very large, e.g., $|\mathcal{C}| \approx 6 \times 10^5$ for the USPTO dataset.

To parameterize the embedding functions f_{θ} , g_{θ} and h_{θ} , we use the recently proposed graph neural network (GNN) architecture, structure2vec (Dai et al., 2016, 2019). The implementation details of the architecture is described in Section 3.1.

Incorporating reaction types. A human expert could have some prior information about a reaction type, e.g., carbon-carbon bond formation, for the target product P . To utilize this prior knowledge, we add trainable embedding bias vectors $u^{(t)}$ and $v^{(t)}$ for each reaction type t into the query embeddings of ψ and ϕ , respectively. For example, $\phi(P|\mathcal{R})$ becomes $\text{CosSim}(\sum_{R \in \mathcal{R}} g_{\theta}(R) + v^{(t)}, h_{\theta}(P))$. The bias vectors are initialized by zero at beginning of training.

2.3 Training scheme with contrastive learning

Finally, we describe our learning scheme for training the score functions defined in Section 2.1 and 2.2. We are inspired by how the score functions $\psi(R|P, \mathcal{R}_{\text{given}})$ and $\phi(P|\mathcal{R})$ resemble the classification scores of selecting (a) the reactant R given the product P and the previously selected reactants $\mathcal{R}_{\text{given}}$ and (b) the product P given all of the selected reactants \mathcal{R} , respectively. Based on this intuition, we consider two classification tasks with the following probabilities:

$$\begin{aligned}p(R|P, \mathcal{R}_{\text{given}}, \mathcal{C}) &= \frac{\exp(\psi(R|P, \mathcal{R}_{\text{given}})/\tau)}{\sum_{R' \in \mathcal{C} \setminus \{P\}} \exp(\psi(R'|P, \mathcal{R}_{\text{given}})/\tau)}, \\ q(P|\mathcal{R}, \mathcal{C}) &= \frac{\exp(\phi(P|\mathcal{R})/\tau)}{\sum_{P' \in \mathcal{C} \setminus \mathcal{R}} \exp(\phi(P'|\mathcal{R})/\tau)},\end{aligned}$$

where τ is a hyperparameter for temperature scaling and \mathcal{C} is the given candidate set of molecules. Note that we do not consider P and $R \in \mathcal{R}$ as available reactants and products for the classification tasks of p and q , respectively. This reflects our prior knowledge that the product P is always different from the reactants \mathcal{R} in a chemical reaction. As a result,

we arrive at the following losses defined on a reaction of the product P and the reactant-set $\mathcal{R} = \{R_1, \dots, R_n\}$:

$$\begin{aligned}\mathcal{L}_{\text{backward}}(P, \mathcal{R}|\theta, \mathcal{C}) &= -\max_{\pi \in \Pi} \sum_{i=1}^{n+1} \log p(R_{\pi(i)}|P, \{R_{\pi(1)}, \dots, R_{\pi(i-1)}\}, \mathcal{C}), \\ \mathcal{L}_{\text{forward}}(P, \mathcal{R}|\theta, \mathcal{C}) &= -\log q(P|\mathcal{R}, \mathcal{C}),\end{aligned}$$

where $R_{n+1} = R_{\text{halt}}$ and Π is the space of permutations defined on the integers $1, \dots, n+1$ satisfying $\pi(n+1) = n+1$. We note that minimizing the above losses increases the scores $\psi(R|P, \mathcal{R}_{\text{given}})$ and $\phi(P|\mathcal{R})$ of the correct pairs of product and reactants, i.e., numerators, while decreasing that of wrong pairs, i.e., denominators. Such an objective is known as contrastive loss which has recently gained much attention in various domains (Sohn, 2016; He et al., 2019; Chen et al., 2020b; Oord et al., 2018; Srinivas et al., 2020).

Unfortunately, the optimization of $\mathcal{L}_{\text{backward}}$ and $\mathcal{L}_{\text{forward}}$ is intractable since the denominators of $p(R|P, \mathcal{R}_{\text{given}}, \mathcal{C})$ and $q(P|\mathcal{R}, \mathcal{C})$ require summation over the large set of candidate molecules \mathcal{C} . To resolve this, for each mini-batch of reactions \mathcal{B} sampled from the training dataset, we approximate \mathcal{C} with the following set of molecules:

$$\mathcal{C}_{\mathcal{B}} = \{M \mid \exists (\mathcal{R}, P) \in \mathcal{B} \text{ such that } M = P \text{ or } M \in \mathcal{R}\},$$

i.e., $\mathcal{C}_{\mathcal{B}}$ is the set of all molecules in \mathcal{B} . Then we arrive at the following training objective:

$$\mathcal{L}(\mathcal{B}|\theta) = \frac{1}{|\mathcal{B}|} \sum_{(\mathcal{R}, P) \in \mathcal{B}} \left(\mathcal{L}_{\text{backward}}(P, \mathcal{R}|\theta, \mathcal{C}_{\mathcal{B}}) + \mathcal{L}_{\text{forward}}(P, \mathcal{R}|\theta, \mathcal{C}_{\mathcal{B}}) \right). \quad (2)$$

Hard negative mining. In our setting, molecules in the candidate set $\mathcal{C}_{\mathcal{B}}$ are easily distinguishable. Hence, learning to discriminate between them is often not informative. To alleviate this issue, we replace the $\mathcal{C}_{\mathcal{B}}$ with its augmented version $\tilde{\mathcal{C}}_{\mathcal{B}}$ by adding *hard* negative samples, i.e., similar molecules, as follows:

$$\tilde{\mathcal{C}}_{\mathcal{B}} = \mathcal{C}_{\mathcal{B}} \cup \bigcup_{M \in \mathcal{C}_{\mathcal{B}}} \{\text{Top-}K \text{ nearest neighbors of } M \text{ from } \mathcal{C}\},$$

where K is a hyperparameter controlling hardness of the contrastive task. The nearest neighbors are defined with respect to the cosine similarity on $\{h_{\theta}(M)\}_{M \in \mathcal{C}}$. Since computing all embeddings $\{h_{\theta}(M)\}_{M \in \mathcal{C}}$ for every iteration is time-consuming, we update information of the nearest neighbors periodically. We found that the hard negative mining plays a significant role in improving the performance of RETCL (see Section 3.3).

3 Experiments

3.1 Experimental setup

Dataset. We mainly evaluate our framework in USPTO-50k, which is a standard benchmark for the task of retrosynthesis. It contains 50k reactions of 10 reaction types derived from the US patent literature, and we divide it into training/validation/test splits following Coley

Table 1: The top- k exact match accuracy (%) of computer-aided approaches in USPTO-50k. The template-based approaches use the knowledge of reaction templates while others do not. [†]The results are reproduced using the code of [Chen et al. \(2019\)](#).

Category	Method	Top-1	Top-3	Top-5	Top-10	Top-20	Top-50
Reaction type is unknown							
Template-free	Transformer (Karpov et al., 2019)	37.9	57.3	62.7	-	-	-
	SCROP (Zheng et al., 2019)	43.7	60.0	65.2	68.7	-	-
	Transformer (Chen et al., 2019)	44.8	62.6	67.7	71.1	-	-
	G2Gs (Shi et al., 2020)	48.9	67.6	72.5	75.5	-	-
Template-based	retrosim (Coley et al., 2017b)	37.3	54.7	63.3	74.1	82.0	85.3
	neuralsym (Segler & Waller, 2017)	44.4	65.3	72.4	78.9	82.2	83.1
	GLN (Dai et al., 2019)	52.5	69.0	75.6	83.7	89.0	92.4
Selection-based	Bayesian-Retro (Guo et al., 2020)	47.5	67.2	77.0	80.3	-	-
	RETCL (Ours)	71.3	86.4	92.0	94.1	95.0	96.4
Reaction type is given as prior							
Template-free	seq2seq (Liu et al., 2017)	37.4	52.4	57.0	61.7	65.9	70.7
	Transformer [†] (Chen et al., 2019)	54.1	70.0	74.2	77.8	80.4	83.3
	SCROP (Zheng et al., 2019)	59.0	74.8	78.1	81.1	-	-
	G2Gs (Shi et al., 2020)	61.0	81.3	86.0	88.7	-	-
Template-based	retrosim (Coley et al., 2017b)	52.9	73.8	81.2	88.1	91.8	92.9
	neuralsym (Segler & Waller, 2017)	55.3	76.0	81.4	85.1	86.5	86.9
	GLN (Dai et al., 2019)	64.2	79.1	85.2	90.0	92.3	93.2
Selection-based	Bayesian-Retro (Guo et al., 2020)	55.2	74.1	81.4	83.5	-	-
	RETCL (Ours)	78.9	90.4	93.9	95.2	95.8	96.7

[et al. \(2017b\)](#). To apply our framework, we choose the candidate set of commercially available molecules \mathcal{C} as the all reactants in the entire USPTO database as [Guo et al. \(2020\)](#) did. This results in the candidate set with a size of 671,518. For the evaluation metric, we use the top- k exact match accuracy, which is widely used in the retrosynthesis literature. We also experiment with other USPTO benchmarks for more challenging tasks, e.g., generalization to unseen templates. We provide a more detailed description of the USPTO benchmarks in Appendix A.

Hyperparameters. We use a single shared 5-layer structure2vec ([Dai et al., 2016, 2019](#)) architecture and three separate 2-layer residual blocks with an embedding size of 256. To obtain graph-level embedding vectors, we use sum pooling over mean pooling since it captures the size information of molecules. For contrastive learning, we use a temperature of $\tau = 0.1$ and $K = 4$ nearest neighbors for hard negative mining. More details are provided in Appendix B.

3.2 Single-step retrosynthesis in USPTO-50k

Table 1 evaluates our RETCL and other baselines using the top- k exact match accuracy with $k \in \{1, 3, 5, 10, 20, 50\}$. We first note that our framework significantly outperforms a concurrent

Table 2: The top- k exact match accuracy (%) of our RETCL, Transformer (Chen et al., 2019) and GLN (Dai et al., 2019) with discarding predictions not in the candidate set \mathcal{C} .

Category	Method	Top-1	Top-5	Top-10	Top-50	Top-100	Top-200
Reaction type is unknown							
Template-free	Transformer (Chen et al., 2019)	59.6	74.3	77.0	79.4	79.5	79.6
	RETCL (Ours)	71.3	92.0	94.1	96.4	96.7	97.1
Template-based	GLN (Dai et al., 2019)	77.3	90.0	92.5	93.3	93.3	93.3
Reaction type is given as prior							
Template-free	Transformer (Chen et al., 2019)	68.4	82.4	84.3	85.9	86.0	86.1
	RETCL (Ours)	78.9	93.9	95.2	96.7	97.1	97.5
Template-based	GLN (Dai et al., 2019)	82.0	91.7	92.9	93.3	93.3	93.3

selection-based approach,² Bayesian-Retro (Guo et al., 2020), by 23.8% and 23.7% in terms of top-1 accuracy when reaction type is unknown and given, respectively. Furthermore, ours also outperforms template-based approaches utilizing the different knowledge, i.e., reaction templates instead of candidates, with a large margin, e.g., 18.8% over GLN (Dai et al., 2019) in terms of top-1 accuracy when reaction type is unknown.

Incorporating the knowledge of candidates into baselines. However, it is hard to fairly compare between methods operating under different assumptions. For example, template-based approaches require the knowledge of reaction templates, while our selection-based approach requires that of available reactants. To alleviate such a concern, we incorporate our prior knowledge of candidates \mathcal{C} into the baselines; we filter out reactants outside the candidates \mathcal{C} from the predictions made by the baselines. As reported in Table 2, our framework still outperforms the template-free approaches with a large margin, e.g., Transformer (Chen et al., 2019) achieves 68.4% in the top-1 accuracy, while we achieve 78.9% when reaction type is given. Although GLN uses more knowledge than ours in this setting, its top- k accuracy is saturated to 93.3% which is the coverage of known templates, i.e., the upper bound of template-based approaches. However, our framework continues to increase the top- k accuracy as k increases, e.g., 97.5% in terms of top-200 accuracy. We additionally compare with SCROP (Zheng et al., 2019) using their publicly available predictions with reaction types; SCROP achieves 70.4% in the top-1 accuracy, which also underperforms ours.

3.3 Analysis and ablation study

Failure cases. Figure 3 shows examples of wrong predictions from our framework. We found that the reactants of wrong predictions are still similar to the ground-truth ones. For example, the top-3 predictions of the examples A and B are partially correct; the larger reactant is correct while the smaller one is slightly different. In the example C, the ring at the center of the product is broken in the ground-truth reactants while our RETCL predicts non-broken reactants. Surprisingly, in a chemical database, Reaxys, we found a synthetic route starting from reactants in the top-2 prediction to synthesize the target product. We

²Note that Bayesian-Retro (Guo et al., 2020) is not scalable to a large candidate set. See Section 4 for details.

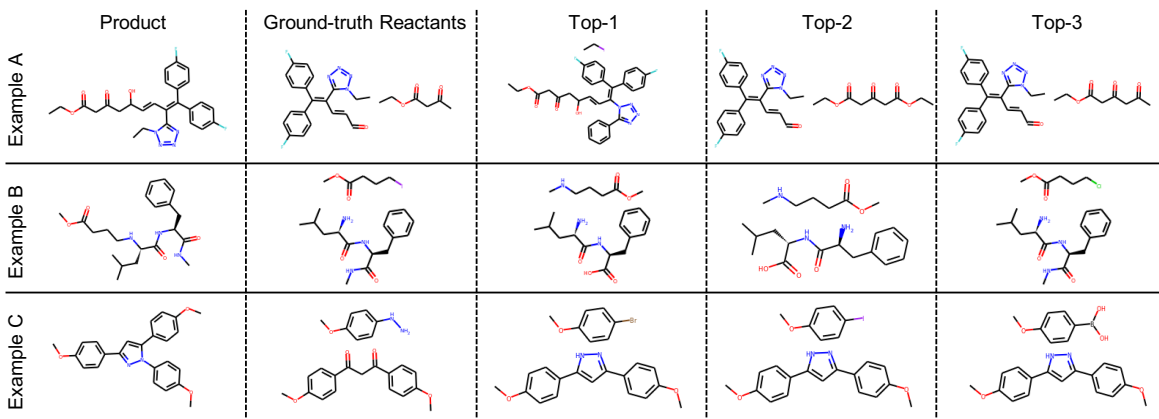


Figure 3: Failure cases of RETCL.

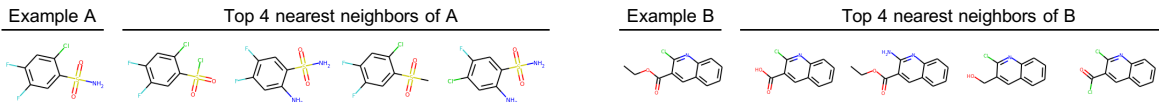


Figure 4: The top-4 nearest neighbors of two randomly sampled molecules in \mathcal{C} .

attach the corresponding route to Appendix C. These results show that our RETCL could provide meaningful information for retrosynthetic analysis in practice.

Nearest neighbors on molecular embeddings. For hard negative mining described in Section 2.3, it is required to find similar molecules using the cosine similarity on $\{h_\theta(M)\}_{M \in \mathcal{C}}$. As illustrated in Figure 4, $h_\theta(M)$ is capable of capturing the molecular structures.

Effect of components. Table 3 shows the effect of components of our framework. First, we found that the hard negative mining as described in Section 2.3 increases the performance significantly. This is because there are many similar molecules in the candidate set \mathcal{C} , thus a model could predict slightly different reactants without hard negative mining. We also demonstrate the effect of checking the synthesizability of the predicted reactants with $\phi(P|\mathcal{R})$. As seen the fourth and fifth rows in Table 3, using $\phi(P|\mathcal{R})$ provides a 2.6% gain in terms of top-10 accuracy. Moreover, we empirically found that **sum** pooling for aggregating node embedding vectors is more effective than **mean** pooling. This is because the former can capture the size of molecules as the norm of graph embedding vectors.

Table 3: Ablation study.

$\phi(P \mathcal{R})$	K	sum	Top-1	Top-10
✓			59.5	79.8
✓	1		69.6	92.2
✓	2		70.9	92.7
✓	4		71.1	92.9
	4		69.8	90.3
✓	4	✓	71.3	94.1

3.4 More challenging retrosynthesis tasks

Generalization to unseen templates. The advantage of our framework over the template-based approaches is the generalization ability to unseen reaction templates. To demonstrate it, we remove reactions of classes (i.e., reaction types) from 6 to 10 in training/validation splits of the USPTO-50k benchmark. Then the number of remaining reactions is 27k. In this

Table 4: The top-10 exact match accuracy (%) of our RETCL and GLN (Dai et al., 2019) trained on USPTO-50k without reaction types from 6 to 10. The average column indicates the average of class-wise accuracy for each reaction type.

Method	Average	Reaction type									
		1	2	3	4	5	6	7	8	9	10
GLN (Dai et al., 2019)	39.7	84.3	92.2	70.7	59.3	89.7	0.0	0.0	0.0	0.5	0.0
RETCL (Ours)	55.6	93.9	97.6	86.4	67.0	95.6	59.1	11.9	18.3	26.1	0.0

case, the templates extracted from the modified dataset cannot be applied to the reactions of different classes. Hence the template-based approaches suffer from the generalization issue; for example, GLN (Dai et al., 2019) cannot provide correct predictions for reactions of unseen types as reported in Table 4, while our RETCL is able to provide correct answers.

We also conduct a more realistic experiment: testing on a larger dataset, the test split of USPTO-full dataset preprocessed by Dai et al. (2019), using a model trained on a smaller dataset, USPTO-50k. We note that the number of reactions for training, 40k, is smaller than that of testing reactions, 100k. As reported in Table 5, our framework provides a consistent benefit over the template-based approaches. These results show that our strength of generalization ability.

Table 5: Generalization to USPTO-full.

Method	Top-1	Top-10	Top-50
Transformer (Chen et al., 2019)	29.9	46.6	51.0
GLN (Dai et al., 2019)	26.7	42.2	46.7
RETCL (Ours)	39.9	57.1	60.9

Generalization to unseen candidates.

The knowledge of the candidate set \mathcal{C} could be updated after learning the RETCL framework. In this case, the set used in the test phase is larger than that in the training

phase, i.e., $\mathcal{C}_{\text{train}} \subsetneq \mathcal{C}_{\text{test}}$. One can learn the framework once again, however someone wants to use it instantly without additional training. To validate that our framework can generalize to unseen candidates, we use a smaller candidate set during the training phase. To be specific, we use all molecules present in training and validation splits of USPTO-50k. In this case, the number of candidate reactants in the training phase is 91297. When testing, we use the original candidate set, in other words, $|\mathcal{C}_{\text{test}}| = 671518$. As reported in Table 6, this model achieves comparable performance to another model trained with a larger number of candidate reactants. This experiment demonstrates that our framework trained with a small corpora (e.g., USPTO-50k) can work with unseen candidates.

Table 6: Generalization to unseen candidates.

$ \mathcal{C}_{\text{train}} $	Top-1	Top-5	Top-10	Top-20	Top-50
91,297	69.0	88.1	91.0	92.8	94.4
671,518	71.3	92.0	94.1	95.0	96.4

Multi-step retrosynthesis. To consider a more practical scenario, we evaluate our algorithm for the task of *multi-step retrosynthesis*. To this end, we use the synthetic route benchmark provided by Chen et al. (2020a). Here, we assume that only the building blocks (or starting materials) are commercially available, and intermediate reactants

require being synthesized from the building blocks. In this challenging task, we demonstrate

Table 7: Multi-step retrosynthesis.

Single-step model	Single		Hybrid	
	MLP	TF	TF+TF	RETCL+TF
Succ. rate (%)	86.84	91.05	90.54	96.84
Avg. length	-	4.30	4.31	3.90

how our method could be used to improve the existing template-free Transformer model (TF, [Chen et al. 2019](#)). Given a target product, the hybrid algorithm operates as follows: (1) our RETCL proposes a set of reactants from the candidates \mathcal{C} ; (2) TF proposes additional reactants outside the candidates \mathcal{C} ; (3) TF chooses the top- K reactants based on its log-likelihood of all the proposed reactants. As an additional baseline, we replace RETCL by another independently trained TF in the hybrid algorithm. We use Retro* ([Chen et al., 2020a](#)) for efficient route search with the retrosynthesis models and evaluate the discovered routes based on the metrics used by [Kishimoto et al. \(2019\)](#); [Chen et al. \(2020a\)](#). As reported in [Table 7](#), our model can enhance the search quality of the existing template-free model in the multi-step retrosynthesis scenarios. This is because our RETCL is able to recommend available and plausible reactants to TF for each retrosynthesis step. Note that the MLP column is the same as reported in [Chen et al. \(2020a\)](#) which uses a template-based single-step MLP model. The detailed description of this multi-step retrosynthesis experiment and the discovered routes are provided in [Appendix D](#).

4 Related work

The template-based approaches ([Coley et al., 2017b](#); [Segler & Waller, 2017](#); [Dai et al., 2019](#)) rely on reaction templates that are extracted from a reaction database ([Coley et al., 2017a, 2019](#)) or encoded by experts ([Szymkuć et al., 2016](#)). They first select one among known templates, and then apply it to the target product. On the other hand, template-free methods ([Liu et al., 2017](#); [Karpov et al., 2019](#); [Zheng et al., 2019](#); [Shi et al., 2020](#)) consider retrosynthesis as a conditional generation problem such as machine translation. Recently, synthon-based approaches ([Shi et al., 2020](#); [Somnath et al., 2020](#)) have also shown the promising results based on utilizing the atom-mapping between products and reactants as an additional type of supervisions.

Concurrent to our work, [Guo et al. \(2020\)](#) also propose a selection-based approach, Bayesian-Retro, based on sequential Monte Carlo sampling ([Del Moral et al., 2006](#)). As reported in [Table 1](#), our RETCL significantly outperforms Bayesian-Retro. The gap is more evident since it uses 6×10^5 forward evaluations (i.e., 6 hours) of Molecular Transformer ([Schwaller et al., 2019](#)) for single-step retrosynthesis of one target product while our RETCL requires only one second.

5 Conclusion

In this paper, we propose RETCL for solving retrosynthesis. To this end, we reformulate retrosynthesis as a selection problem of commercially available reactants, and propose a contrastive learning scheme with hard negative mining to train our RETCL. Through the extensive experiments, we show that our framework achieves outstanding performance for the USPTO benchmarks. Furthermore, we demonstrate the generalizability of RETCL to unseen reaction templates. We believe that extending our framework to multi-step retrosynthesis or combining with various contrastive learning techniques in other domains could be interesting future research directions.

Acknowledgments

This work was mainly supported by Samsung Electronics Co., Ltd (IO201211-08107-01) and Institute of Information & Communications Technology Planning & Evaluation (IITP) grant funded by the Korea government (MSIT) (No.2019-0-00075, Artificial Intelligence Graduate School Program (KAIST)).

References

- Benson Chen, Tianxiao Shen, Tommi S Jaakkola, and Regina Barzilay. Learning to make generalizable and diverse predictions for retrosynthesis. *arXiv preprint arXiv:1910.09688*, 2019.
- Binghong Chen, Chengtao Li, Hanjun Dai, and Le Song. Retro*: Learning retrosynthetic planning with neural guided a* search. In *ICML, 2020a*.
- Ting Chen, Simon Kornblith, Mohammad Norouzi, and Geoffrey Hinton. A simple framework for contrastive learning of visual representations. *arXiv preprint arXiv:2002.05709*, 2020b.
- Connor W Coley, Regina Barzilay, Tommi S Jaakkola, William H Green, and Klavs F Jensen. Prediction of organic reaction outcomes using machine learning. *ACS central science*, 3(5): 434–443, 2017a.
- Connor W Coley, Luke Rogers, William H Green, and Klavs F Jensen. Computer-assisted retrosynthesis based on molecular similarity. *ACS central science*, 3(12):1237–1245, 2017b.
- Connor W Coley, William H Green, and Klavs F Jensen. Rdcchiral: An rdkit wrapper for handling stereochemistry in retrosynthetic template extraction and application. *Journal of chemical information and modeling*, 59(6):2529–2537, 2019.
- Elias James Corey. The logic of chemical synthesis: multistep synthesis of complex carbogenic molecules (nobel lecture). *Angewandte Chemie International Edition in English*, 30(5): 455–465, 1991.
- Elias James Corey, Alan K Long, and Steward D Rubenstein. Computer-assisted analysis in organic synthesis. *Science*, 228(4698):408–418, 1985.
- Hanjun Dai, Bo Dai, and Le Song. Discriminative embeddings of latent variable models for structured data. In *International conference on machine learning*, pp. 2702–2711, 2016.
- Hanjun Dai, Chengtao Li, Connor Coley, Bo Dai, and Le Song. Retrosynthesis prediction with conditional graph logic network. In H. Wallach, H. Larochelle, A. Beygelzimer, F. d'Alché-Buc, E. Fox, and R. Garnett (eds.), *Advances in Neural Information Processing Systems 32*, pp. 8872–8882. Curran Associates, Inc., 2019.
- Pierre Del Moral, Arnaud Doucet, and Ajay Jasra. Sequential monte carlo samplers. *Journal of the Royal Statistical Society: Series B (Statistical Methodology)*, 68(3):411–436, 2006.

- Zsombor Gonda and Zoltan Novak. Transition-metal-free n-arylation of pyrazoles with diaryliodonium salts. *Chemistry (Weinheim an der Bergstrasse, Germany)*, 21(47):16801–16806, 2015.
- Zhongliang Guo, Stephen Wu, Mitsuru Ohno, and Ryo Yoshida. A bayesian algorithm for retrosynthesis. *arXiv preprint arXiv:2003.03190*, 2020.
- Ben Harwood, BG Kumar, Gustavo Carneiro, Ian Reid, Tom Drummond, et al. Smart mining for deep metric learning. In *Proceedings of the IEEE International Conference on Computer Vision*, pp. 2821–2829, 2017.
- Kaiming He, Haoqi Fan, Yuxin Wu, Saining Xie, and Ross Girshick. Momentum contrast for unsupervised visual representation learning. *arXiv preprint arXiv:1911.05722*, 2019.
- Olivier J Hénaff, Aravind Srinivas, Jeffrey De Fauw, Ali Razavi, Carl Doersch, SM Eslami, and Aaron van den Oord. Data-efficient image recognition with contrastive predictive coding. *arXiv preprint arXiv:1905.09272*, 2019.
- Pavel Karpov, Guillaume Godin, and Igor V Tetko. A transformer model for retrosynthesis. In *International Conference on Artificial Neural Networks*, pp. 817–830. Springer, 2019.
- Akihiro Kishimoto, Beat Buesser, Bei Chen, and Adi Botea. Depth-first proof-number search with heuristic edge cost and application to chemical synthesis planning. In *Advances in Neural Information Processing Systems*, pp. 7226–7236, 2019.
- Kangjie Lin, Youjun Xu, Jianfeng Pei, and Luhua Lai. Automatic retrosynthetic pathway planning using template-free models. *arXiv preprint arXiv:1906.02308*, 2019.
- Bowen Liu, Bharath Ramsundar, Prasad Kawthekar, Jade Shi, Joseph Gomes, Quang Luu Nguyen, Stephen Ho, Jack Sloane, Paul Wender, and Vijay Pande. Retrosynthetic reaction prediction using neural sequence-to-sequence models. *ACS central science*, 3(10): 1103–1113, 2017.
- Daniel Mark Lowe. *Extraction of chemical structures and reactions from the literature*. PhD thesis, University of Cambridge, 2012.
- Troy Mutton and Damon D Ridley. Understanding similarities and differences between two prominent web-based chemical information and data retrieval tools: Comments on searches for research topics, substances, and reactions. *Journal of Chemical Education*, 96(10): 2167–2179, 2019.
- Aaron van den Oord, Yazhe Li, and Oriol Vinyals. Representation learning with contrastive predictive coding. *arXiv preprint arXiv:1807.03748*, 2018.
- Adam Paszke, Sam Gross, Soumith Chintala, Gregory Chanan, Edward Yang, Zachary DeVito, Zeming Lin, Alban Desmaison, Luca Antiga, and Adam Lerer. Automatic differentiation in pytorch. In *NIPS 2017 Autodiff Workshop*, 2017.
- Nadine Schneider, Nikolaus Stiefl, and Gregory A Landrum. What’s what: The (nearly) definitive guide to reaction role assignment. *Journal of chemical information and modeling*, 56(12):2336–2346, 2016.

- Philippe Schwaller, Teodoro Laino, Théophile Gaudin, Peter Bolgar, Christopher A Hunter, Costas Bekas, and Alpha A Lee. Molecular transformer: A model for uncertainty-calibrated chemical reaction prediction. *ACS central science*, 5(9):1572–1583, 2019.
- Marwin HS Segler and Mark P Waller. Neural-symbolic machine learning for retrosynthesis and reaction prediction. *Chemistry—A European Journal*, 23(25):5966–5971, 2017.
- Chence Shi, Minkai Xu, Hongyu Guo, Ming Zhang, and Jian Tang. A graph to graphs framework for retrosynthesis prediction. *arXiv preprint arXiv:2003.12725*, 2020.
- Kihyuk Sohn. Improved deep metric learning with multi-class n-pair loss objective. In D. D. Lee, M. Sugiyama, U. V. Luxburg, I. Guyon, and R. Garnett (eds.), *Advances in Neural Information Processing Systems 29*, pp. 1857–1865. Curran Associates, Inc., 2016.
- Vignesh Ram Somnath, Charlotte Bunne, Connor W Coley, Andreas Krause, and Regina Barzilay. Learning graph models for template-free retrosynthesis. *arXiv preprint arXiv:2006.07038*, 2020.
- Aravind Srinivas, Michael Laskin, and Pieter Abbeel. Curl: Contrastive unsupervised representations for reinforcement learning. *arXiv preprint arXiv:2004.04136*, 2020.
- Sara Szymkuć, Ewa P Gajewska, Tomasz Klucznik, Karol Molga, Piotr Dittwald, Michał Startek, Michał Bajczyk, and Bartosz A Grzybowski. Computer-assisted synthetic planning: The end of the beginning. *Angewandte Chemie International Edition*, 55(20):5904–5937, 2016.
- Yonglong Tian, Dilip Krishnan, and Phillip Isola. Contrastive multiview coding. *arXiv preprint arXiv:1906.05849*, 2019.
- Minjie Wang, Lingfan Yu, Da Zheng, Quan Gan, Yu Gai, Zihao Ye, Mufei Li, Jinjing Zhou, Qi Huang, Chao Ma, et al. Deep graph library: Towards efficient and scalable deep learning on graphs. *arXiv preprint arXiv:1909.01315*, 2019.
- David Weininger. Smiles, a chemical language and information system. 1. introduction to methodology and encoding rules. *Journal of chemical information and computer sciences*, 28(1):31–36, 1988.
- Shuangjia Zheng, Jiahua Rao, Zhongyue Zhang, Jun Xu, and Yuedong Yang. Predicting retrosynthetic reactions using self-corrected transformer neural networks. *Journal of Chemical Information and Modeling*, 2019.

A Dataset details

We here describe the details of USPTO datasets. The reactions in the USPTO datasets are derived from the US patent literature (Lowe, 2012). The entire set, USPTO 1976-2016, contains 1.8 million raw reactions. The commonly-used benchmark of single-step retrosynthesis is USPTO-50k containing 50k clean atom-mapped reactions which can be classified into 10 broad reaction types (Schneider et al., 2016). See Table 8a for the information of the reaction types. For generalization experiments in Section 3.4, we introduce a filtered dataset, USPTO-50k-modified, which contains reactions of reaction types from 1 to 5. We report the number of reactions of the modified dataset in Table 8b. We also use the USPTO-full dataset, provided by Dai et al. (2019), which contains 1.1 million reactions. Note that we use only the test split of USPTO-full (i.e., only 101k reactions) for testing generalizability. Note that we do not use atom-mappings in the USPTO benchmarks. Moreover, we do not consider reagents for single-step retrosynthesis following prior work (Liu et al., 2017; Dai et al., 2019; Lin et al., 2019; Karpov et al., 2019).

Table 8: The detailed information on USPTO datasets.

(a) The information about reaction types in USPTO-50k.			(b) The number of reactions in datasets.		
ID	Fraction (%)	Description	Dataset	Split	#
1	30.3	heteroatom alkylation and arylation	USPTO-50k	Train	40,008
2	23.8	acylation and related processes		Val	5,001
3	11.3	C-C bond formation		Test	5,007
4	1.8	heterocycle formation	USPTO-50k-modified	Train	27,429
5	1.3	protections		Val	3,429
6	16.5	deprotections		Test	5,007
7	9.2	reductions	USPTO-full	Train	810,496
8	1.6	oxidations		Val	101,311
9	3.7	functional group interconversion (FGI)		Test	101,311
10	0.5	functional group addition (FGA)			

B Implementation details

We here provide a detailed description of our implementation. Since the USPTO datasets provide molecule information based on the SMILES (Weininger, 1988) format, we convert a SMILES representation to a bidirectional graph with atom and bond features. To this end, we use RDKit³ and Deep Graph Library (DGL) (Wang et al., 2019). Let $G = (V, E)$ be the molecular graph, and $X(v) \in \mathbb{R}^{d_{\text{atom}}}$ and $X(uv) \in \mathbb{R}^{d_{\text{bond}}}$ are features for an atom $v \in V$ and a bond $uv \in E$ in the molecular graph G , respectively. The atom feature $X(v)$ includes the atom type (e.g., C, I, B), degree, formal charge, and so on; the bond feature $X(uv)$ includes the bond type (single, double, triple or aromatic), whether the bond is in a ring, and so on. For more details, we highly recommend to see DGL and its extension, DGL-LifeSci.⁴

Architecture. We build our graph neural network (GNN) architecture based on the molecular

³Open-Source Cheminformatics Software, <https://www.rdkit.org/>

⁴Bringing Graph Neural Networks to Chemistry and Biology, <https://lifesci.dgl.ai/>

graph G with features X as follows:

$$\begin{aligned} H^{(0)}(v) &\leftarrow \text{ReLU} \left(\text{BN} \left(W_{\text{atom}}^{(0)} X(v) + \sum_{u \in \mathcal{N}(v)} W_{\text{bond}}^{(0)} X(uv) \right) \right), \\ H^{(l)}(v) &\leftarrow \text{ReLU} \left(\text{BN} \left(W_1^{(l)} \sum_{u \in \mathcal{N}(v)} H^{(l-1)}(u) + \sum_{u \in \mathcal{N}(v)} W_{\text{bond}}^{(l)} X(uv) \right) \right), \\ H^{(l)}(v) &\leftarrow \text{ReLU} \left(\text{BN} \left(W_2^{(l)} H^{(l)}(v) + H^{(l-1)}(v) \right) \right), \text{ for } l = 1, 2, \dots, L, \\ H(v) &\leftarrow W_{\text{last}} H^{(L)}(v), \end{aligned}$$

where $\mathcal{N}(v)$ is the set of adjacent vertices with v . This architecture is based on structure2vec (Dai et al., 2019, 2016), however it is slightly different with the model used by Dai et al. (2019): we use ReLU after BN instead of BN after ReLU; we append a last linear model W_{last} . Based on the atom-level embeddings $H(v)$, we construct query and key embeddings f_θ , g_θ , and h_θ using three separate residual blocks as follows:

$$\begin{aligned} f_\theta(M) &\leftarrow \sum_{v \in V} \left(H(v) + \text{BN}(W_2^{(f)} \text{ReLU}(\text{BN}(W_1^{(f)} \text{ReLU}(H(v)))) \right), \\ g_\theta(M) &\leftarrow \sum_{v \in V} \left(H(v) + \text{BN}(W_2^{(g)} \text{ReLU}(\text{BN}(W_1^{(g)} \text{ReLU}(H(v)))) \right), \\ h_\theta(M) &\leftarrow \sum_{v \in V} \left(H(v) + \text{BN}(W_2^{(h)} \text{ReLU}(\text{BN}(W_1^{(h)} \text{ReLU}(H(v)))) \right), \end{aligned}$$

where M is the corresponding molecule with the molecular graph G . Note that θ includes all W defined above, and we omit bias vectors of the linear layers due to the notational simplicity. We found that these design choices, e.g., sharing GNN layers and using residual layers, also provide an accuracy gain. Therefore, more sophisticated architecture designs could provide further improvements; we leave it for future work.

Optimization. For learning the parameter θ , we use the stochastic gradient descent (SGD) with a learning rate of 0.01, a momentum of 0.9, a weight decay of 10^{-5} , a batch size of 64, and a gradient clip of 5.0. We train our model for 200k iterations and evaluate on the validation split every 1000 iterations. The information of the nearest neighbors is also updated every 1000 iterations. When evaluating on the test split, we use the best validation model with a beam size of 200.

To sum up, we use Pytorch (Paszke et al., 2017) for automatic differentiation, Deep Graph Library (Wang et al., 2019) for building graph neural networks, and RDKit for processing SMILES (Weininger, 1988) representations. All our models can be executed on single NVIDIA RTX 2080 Ti GPU.

C Failure case study

As illustrated in Figure 5, we found that our RETCL’s prediction differs from the ground-truth reactants in USPTO-50k, however, it exists as a 3-step reaction with two reagents (sodium acetate and thiophene) in the chemical literature (Gonda & Novak, 2015).⁵ Note that our

⁵We found this synthetic path and the corresponding literature from a chemical database, Reaxys. Note that the sodium acetate and the thiophene are considered as reagents in Reaxys.

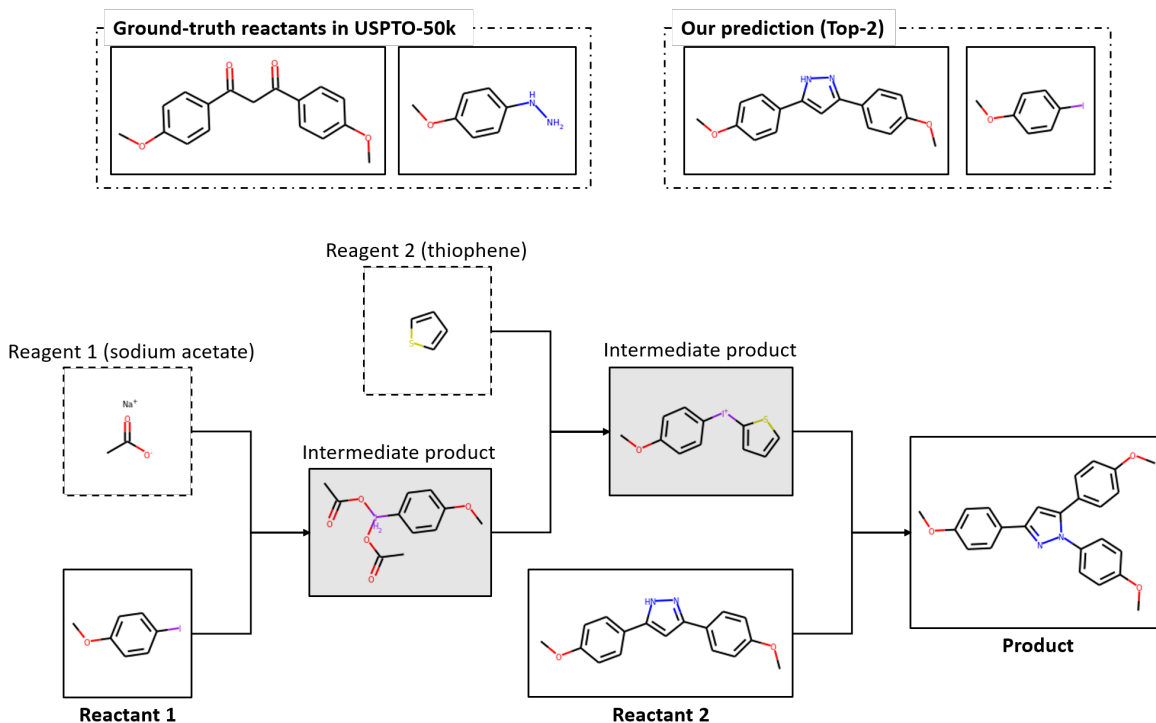


Figure 5: A synthetic path existing in Reaxys based on RETCL’s prediction.

framework currently does not consider reagent prediction. Therefore, our prediction can be regarded as an available (i.e., correct) synthetic path in practice.

D Multi-step retrosynthesis

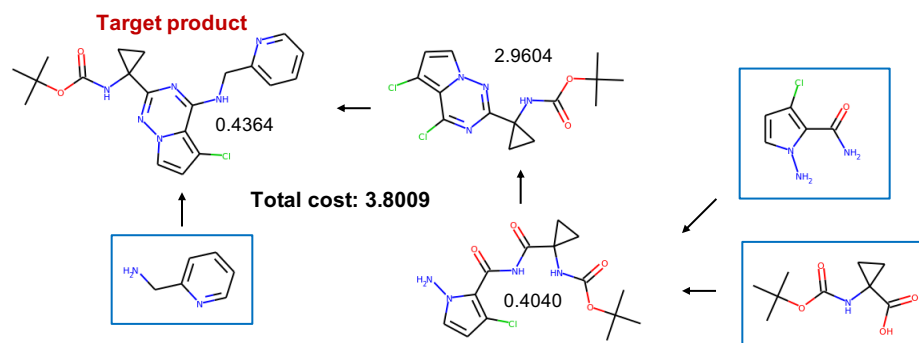
For the multi-step retrosynthesis experiment described in Section 3.4, we use a synthetic route dataset provided by Chen et al. (2020a). This dataset is constructed from the USPTO (Lowe, 2012) database like other benchmarks. We recommend to see Chen et al. (2020a) for the construction details. The dataset contains 299202 training routes, 65274 validation routes, and 190 test routes. We first extract single-step reactions and molecules from the training and validation splits of the dataset. The extracted reactions are used for training our RETCL and Transformer (TF, Chen et al. 2019), and the molecules are used as the candidate set $\mathcal{C}_{\text{train}}$ ⁶ for ours. When testing the single-step models with Retro* (Chen et al., 2020a), we use all starting molecules (i.e., 114802 molecules) in the routes in the dataset as the candidate set \mathcal{C} . This reflects more practical scenarios because intermediate reactants often be unavailable in multi-step retrosynthesis. We remark that TF also uses the candidate set \mathcal{C} as the prior knowledge for finishing the search procedure.

The evaluation metrics used in Section 3.4 are *success rate* and *average length of routes*. The success means that a synthetic route for a target product is successfully discovered under a limit of the number of expansions. We set the limit by 100 and use only the top-5 predictions

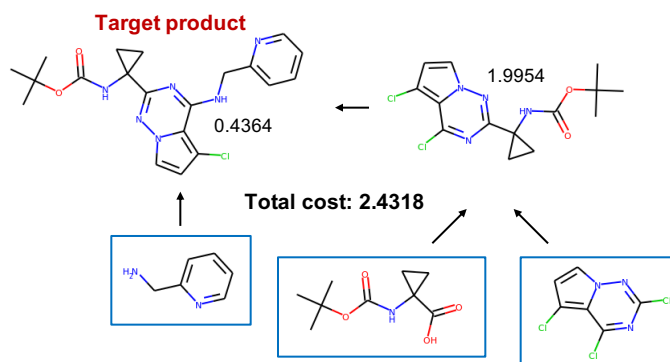
⁶Note that this candidate set is used only for training.

of a single or hybrid model for each expansion. When computing the average length, we only consider the cases where all the single-step models discover routes successfully. As [Chen et al. \(2020a\)](#) did, we use the negative log-likelihood computed by TF as the reaction cost.

Figure 6 and 7 illustrate the discovered routes by TF and RETCL+TF under the aforementioned setting. The molecules in the blue boxes are building blocks (i.e., available reactants) and the numbers indicate the reaction costs (i.e., the negative log-likelihoods computed by TF). As shown in the figures, our algorithm allows to discover a shorter and cheaper route.

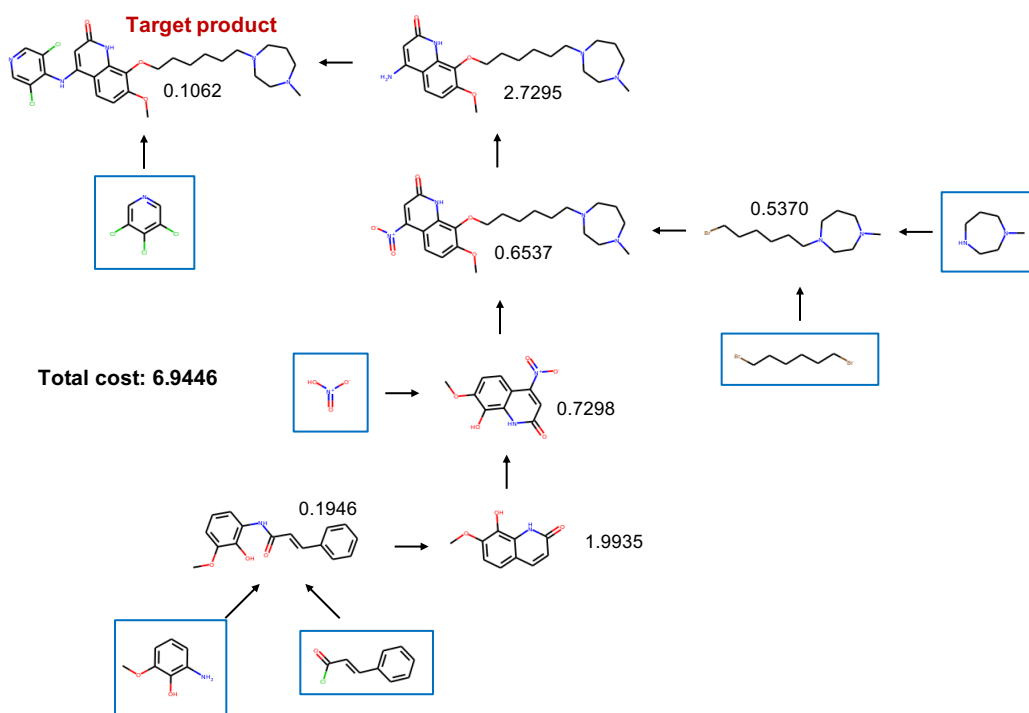


(a) Transformer

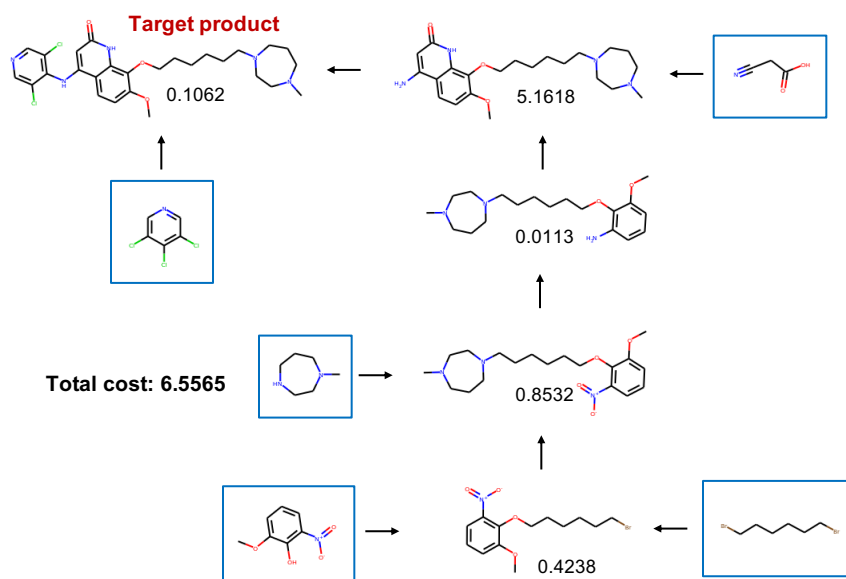


(b) RETCL+Transformer (ours)

Figure 6: Synthetic routes discovered by (a) Transformer and (b) our RETCL+Transformer.



(a) Transformer



(b) RETCL+Transformer (ours)

Figure 7: Synthetic routes discovered by (a) Transformer and (b) our RETCL+Transformer.